



19 – 20 June 2012  
Brussels, Belgium

**Military Green 2012**  
Conference-Exhibition-Demonstration  
Call for Exhibits and Demonstrations



## Methanol Steam Reformer – High Temperature PEM Fuel Cell System Analysis

Andrej LOTRIČ (Mebius d.o.o., Na jami 3, SI-1000 Ljubljana, Slovenia) and Stanko HOČEVAR (Mebius d.o.o., Na jami 3, SI-1000 Ljubljana, Slovenia and National Institute of Chemistry, Lab. Catal. & Chem.React.Eng., Hajdrihova 19, SI-1000 Ljubljana, Slovenia)

The implementation of a high-temperature PEMFC stack into a combined system with a steam methanol reformer (SMR) has been studied. Comparison of efficiency between systems with a high temperature (HT) PEMFC stack and a classical, low-temperature (LT) PEMFC stack has been made. In both systems the methanol reformer operates at 250 °C and steam-to-methanol ratio of 1.5. Classical PEMFC stack operates at 90 °C while high-temperature PEMFC stack operates at 250 °C. Additionally, the system with a classical PEMFC stack uses a catalytic burner to supply the endothermic reforming process with sufficient heat. Partial heat regeneration has been also used in this system because hot exhaust gases from the reformer need to be cooled down before entering the fuel cell stack. Modelling of both systems and sensitivity analysis was performed in Aspen Plus. The results show that efficiency of approximately 54% (based on higher heating value) can be reached with the HT PEMFC system, which is more than 40% higher efficiency compared to the LT PEMFC system.

### 1 Introduction

One of the major constraints for the PEMFC is that they use hydrogen as a fuel which has a very low energy density per volume at conditions of standard ambient pressure and temperature (SAPT). Therefore hydrogen is stored either as gas at very high pressures (up to 800 bar) or as liquid at very low temperatures below -253 °C. As an alternative the reforming of liquid fuels (fossil or renewable) is showing promise because they have much higher energy density per volume. For small portable applications methanol shows good potential because it is sulphur free, has a high hydrogen-to-carbon ratio in its composition and is in liquid form at SAPT, which greatly facilitates its storage and transportation. It can be seen from Table 1 that at SAPT methanol has more than thousand times greater energy density per volume compared to hydrogen.

Table 1: Higher heating value (HHV) of hydrogen at different conditions and methanol at SAPT

Hydrogen		Methanol	Ratio
141.9 kJ/g		20.0 kJ/g	7.1 : 1
SAPT	11.5 kJ/L	15.7 MJ/L	1 : 1,365
800 bar	6.0 MJ/L		1 : 2.6
-253 °C	10.1 MJ/L		1 : 1.6

Another shortcoming of PEMFC is that the heat released during the electrochemical reaction is on relatively low temperature level and it is mostly discarded as waste heat. This is one of the main

reasons that the research is also starting to focus on the so called high-temperature PEMFC, which could operate at temperatures higher than 200 °C. This would allow the reaction kinetics to proceed faster and consequently raise the efficiency of PEMFC and at the same time allow the use of waste heat in cogeneration for different applications.

As it turns out, raising the temperature above 200 °C would have another advantage. The reformat gas exiting the steam reformer always contains some carbon monoxide (CO) which is the main inhibitor of electrochemical reaction in PEMFC. The reason for that is the preferential adsorption of CO onto the active sites of the platinum (Pt) catalyst. At higher temperatures this occurs at a much lesser extent and the HT PEMFC operating above 200 °C could work normally at concentrations higher than 2% of CO in the inlet gas (based on [1]). With good design of the steam reformer such composition of the reformat gas is not too difficult to achieve. This would also remove the need for downstream hydrogen purification processes (WGSR, ProX or methanation) and reduce the costs substantially.

Increasing the temperature of PEMFC operation above 250 °C would have an additional benefit because the heat released during the electrochemical reaction would be on a sufficiently high level to support steam reforming of methanol. The steam reforming process can achieve practically 100% conversion of methanol at temperatures between 250 °C – 300 °C. This depends on the design of reformer. The integrated system with such HT PEMFC stack would have higher efficiency compared to the LT PEMFC because it would not need a catalytic burner to supply continuously the SMR with additional heat for the reforming of methanol.

## **2 System modelling**

Modelling of the SMR was based on the kinetic model proposed by Peppley et al [2]. The kinetics was included directly into Aspen plus using the R-Plug model unit with Langmuir-Hinshelwood kinetic model.

The model of a PEMFC was based on calculations from an in-house developed model in SIMULINK. The results from SIMULINK model were integrated into Aspen Plus User-2 model of PEMFC downloaded from Aspen support site.

### **2.1 Methanol reformer**

To describe properly the methanol conversion as a function of temperature we have used the kinetic model proposed by Peppley et al [2]. The same kinetic model was also used in a study made by Pattekar and Kothare [3] and in a study made by Telotte et al [4]. Comparing all the articles there were some minor mistakes found in equations and some discrepancies in parameters. The values used in our model of the SMR are presented on Figure 1.

The kinetic model presumes that in the SMR three reactions proceed simultaneously: steam methanol reforming (Eq. (1)), direct decomposition of methanol (Eq. (2)), and water gas shift reaction (Eq. (3)):





The rate of reaction  $r_i$  depends on the rate limiting step in its set of elementary reaction steps. The process of steam reforming is a combination of all three reaction sets therefore it is given in the form of the following equations:

$$r_R = \frac{k_R \cdot K_{\text{CH}_3\text{O}(1)}^* \left( \frac{p_{\text{CH}_3\text{OH}}}{p_{\text{H}_2}} \right) \left( 1 - \frac{p_{\text{H}_2}^3 \cdot p_{\text{CO}_2}}{K_R \cdot p_{\text{CH}_3\text{OH}} \cdot p_{\text{H}_2\text{O}}} \right) \cdot C_{S_1}^T \cdot C_{S_{1a}}^T \cdot S_C \cdot \rho_b}{\left( 1 + K_{\text{CH}_3\text{O}(1)}^* \left( \frac{p_{\text{CH}_3\text{OH}}}{p_{\text{H}_2}} \right) + K_{\text{HCOO}(1)}^* \cdot p_{\text{CO}_2} \cdot p_{\text{H}_2}^{1/2} + K_{\text{OH}(1)}^* \left( \frac{p_{\text{H}_2\text{O}}}{p_{\text{H}_2}} \right) \right) + \left( 1 + K_{\text{H}(1a)}^{1/2} \cdot p_{\text{H}_2}^{1/2} \right)}, \quad (4)$$

$$r_D = \frac{k_D \cdot K_{\text{CH}_3\text{O}(2)}^* \left( \frac{p_{\text{CH}_3\text{OH}}}{p_{\text{H}_2}} \right) \left( 1 - \frac{p_{\text{H}_2}^2 \cdot p_{\text{CO}}}{K_D \cdot p_{\text{CH}_3\text{OH}}} \right) \cdot C_{S_2}^T \cdot C_{S_{2a}}^T \cdot S_C \cdot \rho_b}{\left( 1 + K_{\text{CH}_3\text{O}(2)}^* \left( \frac{p_{\text{CH}_3\text{OH}}}{p_{\text{H}_2}} \right) + K_{\text{OH}(2)}^* \left( \frac{p_{\text{H}_2\text{O}}}{p_{\text{H}_2}} \right) \right) + \left( 1 + K_{\text{H}(2a)}^{1/2} \cdot p_{\text{H}_2}^{1/2} \right)}, \quad (5)$$

$$r_W = \frac{k_W \cdot K_{\text{OH}(1)}^* \left( \frac{p_{\text{CO}} \cdot p_{\text{H}_2\text{O}}}{p_{\text{H}_2}} \right) \left( 1 - \frac{p_{\text{H}_2} \cdot p_{\text{CO}_2}}{K_W \cdot p_{\text{CO}} \cdot p_{\text{H}_2\text{O}}} \right) \cdot C_{S_1}^T \cdot S_C \cdot \rho_b}{\left( 1 + K_{\text{CH}_3\text{O}(1)}^* \left( \frac{p_{\text{CH}_3\text{OH}}}{p_{\text{H}_2}} \right) + K_{\text{HCOO}(1)}^* \cdot p_{\text{CO}_2} \cdot p_{\text{H}_2}^{1/2} + K_{\text{OH}(1)}^* \left( \frac{p_{\text{H}_2\text{O}}}{p_{\text{H}_2}} \right) \right)^2}, \quad (6)$$

Eqs. (4)-(6) were used in Aspen Plus process modelling software where R-Plug model unit was used as a SMR. The reactions were integrated into the unit in the form of Langmuir-Hinshelwood kinetics. The reactor is modelled as a plug flow tubular reactor which means that there is no change of thermodynamic properties in radial direction (no concentration, temperature and pressure gradients) but the changes exist in the axial direction. The reactor is designed as a tube of 150 mm length and 10 mm diameter.

## 2.2 Fuel Cell Stack

The efficiency of PEMFC  $\eta$  depends on the generated current density  $j$ , which is directly proportional to the molar flow of used reactants  $\dot{n}$  via the Faraday's law of electrolysis:

$$\dot{n} = \frac{I}{z \cdot F} = \frac{j \cdot A}{z \cdot F}, \quad (7)$$

where  $I$  represents electrical current,  $A$  active surface area of PEMFC,  $z$  number of charge carriers and  $F$  Faraday's constant. In general, the efficiency of an energy system is defined as a ratio between energy supplied to the system and energy produced by the system. In terms of PEMFC the efficiency can be deduced as:

$$\eta = \frac{P_{\text{out}}}{P_{\text{in}}} = \frac{I \cdot U}{\dot{n} \cdot \Delta H_{\text{HHV}}} = \frac{2 \cdot F \cdot U(I)}{\Delta H_{\text{HHV}}}, \quad (8)$$

where  $\Delta H_{HHV}$  is higher heating value of hydrogen and  $U(l)$  fuel cell voltage. From Eq. (7) one can conclude that  $U(l)$  can also be seen as a function of hydrogen molar flow and the efficiency can also be expressed as a function of hydrogen molar flow.

Parameter	Value
$k_R$	$7.4 \times 10^{14} \exp(-102800/(RT)) \text{ m}^2/\text{mol.s}$
$k_D$	$3.8 \times 10^{20} \exp(-170000/(RT)) \text{ m}^2/\text{mol.s}$
$k_W$	$5.9 \times 10^{13} \exp(-87600/(RT)) \text{ m}^2/\text{mol.s}$
$K_R$	$10(1.4142 \times 10^{-13} T^5 - 4.2864 \times 10^{-10} T^4 + 5.3993 \times 10^{-7} T^3 - 3.6385 \times 10^{-4} T^2 + 1.4096 \times 10^{-1} T - 2.0258 \times 10^1) \text{ bar}^2$
$K_D$	$10(2.9463 \times 10^{-13} T^5 - 8.8919 \times 10^{-10} T^4 + 11.1130 \times 10^{-6} T^3 - 7.4160 \times 10^{-4} T^2 + 2.7969 \times 10^{-1} T - 4.4044 \times 10^1) \text{ bar}$
$K_W$	$10(-1.4936 \times 10^{-13} T^5 + 4.5026 \times 10^{-10} T^4 - 5.6216 \times 10^{-7} T^3 + 3.7206 \times 10^{-4} T^2 - 1.3726 \times 10^{-1} T + 2.4537 \times 10^1)$
$K_{CH_3O(1)}^*$	$\exp(-41.8/R - (-20000/(RT))) \text{ bar}^{-0.5}$
$K_{CH_3O(2)}^*$	$\exp(30/R - (-20000/(RT))) \text{ bar}^{-0.5}$
$K_{HCOO(1)}^*$	$\exp(179200/R - (100000/(RT))) \text{ bar}^{-1.5}$
$K_{OH(1)}^*$	$\exp(-44.5/R - (-20000/(RT))) \text{ bar}^{-0.5}$
$K_{OH(2)}^*$	$\exp(30/R - (-20000/(RT))) \text{ bar}^{-0.5}$
$K_{H(1a)}$	$\exp(-100.8/R - (-50000/(RT))) \text{ bar}^{-1}$
$K_{H(2a)}$	$\exp(-46.2/R - (-50000/(RT))) \text{ bar}^{-1}$
$C_{S_1}^T$	$7.5 \times 10^{-6} \text{ mol}/\text{m}^2$
$C_{S_1^a}^T$	$1.5 \times 10^{-5} \text{ mol}/\text{m}^2$
$C_{S_2}^T$	$7.5 \times 10^{-6} \text{ mol}/\text{m}^2$
$C_{S_2^a}^T$	$1.5 \times 10^{-5} \text{ mol}/\text{m}^2$

Reactor Parameter	Value
Catalyst density, $\rho_b$	$1300 \text{ kg}/\text{m}^3$
Specific surface area, $S_C$	$102000 \text{ m}^2/\text{kg}$

Figure 1: Parameters used in the model of SMR

A model of PEMFC stack was downloaded From Aspen Plus support site. It is based on User-2 model unit where a user subroutine is written in Fortran programming language. The programming code was modified in such a way that the efficiency of the PEMFC stack changes in accordance with incoming hydrogen molar flow in a form of a 6th degree polynomial (Graph 1). The polynomial was fitted to the results of 1D model calculated in SIMULINK.

The model of PEMFC in SIMULINK calculates the reversible voltage  $E$  according to the Nernst equation:

$$E = E_0 + \frac{\Delta S}{z \cdot F} (T - T_0) + \frac{R \cdot T}{z \cdot F} \cdot \ln \left( \frac{p_{H_2} \cdot p_{O_2}^{1/2}}{p_{H_2O}} \right), \quad (9)$$

where  $E_0$  is the reversible voltage at SAPT,  $\Delta S$  is the change in reaction enthalpy (for PEMFC it is negative),  $z$  is the number of charge carriers,  $F$  Faraday's constant,  $T$  temperature,  $T_0$  temperature at SAPT,  $R$  universal gas constant and  $p_i$  partial pressure of component  $i$ .

There are several factors that affect the reversible voltage in form of losses. Three major types of losses occur in PEMFC as a result of slow kinetics on electrodes (activation losses), depletion of reactant concentrations due to mass transport (concentration losses) and poor conductivity of protons through the polymer membrane (ohmic losses). These losses are subtracted from the reversible cell potential to obtain the characteristic polarisation curve of the PEMFC.

The kinetics of electrochemical reaction in PEMFC is described by the Butler-Volmer equation:

$$j = j_0 \cdot \left( e^{\frac{\alpha \cdot z \cdot F \cdot \eta_{act}}{R \cdot T}} - e^{\frac{-(1-\alpha) \cdot z \cdot F \cdot \eta_{act}}{R \cdot T}} \right), \quad (10)$$

where  $\alpha$  is the transfer coefficient and  $\eta_{act}$  are the activation losses. If it is assumed that  $\alpha = \frac{1}{2}$  the Euler equation can be used and activation losses can be deduced as:

$$\eta_{act} = \frac{2 \cdot R \cdot T}{z \cdot F} \cdot \operatorname{arcsinh} \left( \frac{j}{j_0} \right), \quad (11)$$

where  $j$  is the current density of PEMFC and  $j_0$  the exchange current density. The contribution to activation losses is only calculated on the cathode side because the kinetics on the cathode side is much slower than that on the anode side. The same situation stands for the concentration losses, which are far greater on the cathode side than on the anode side, especially when air is used as an oxidant. Concentration losses  $\eta_{conc}$  are calculated as:

$$\eta_{conc} = \frac{R \cdot T}{z \cdot F} \cdot \left( 1 + \frac{1}{\alpha} \right) \cdot \ln \left( \frac{j_L}{j_L - j} \right), \quad (12)$$

where  $j_L$  is the limiting current of the PEMFC. Ohmic losses  $\eta_{ohm}$  are defined according to Ohm's law and can be written as:

$$\eta_{ohm} = j \cdot \frac{d}{A \cdot \sigma}, \quad (13)$$

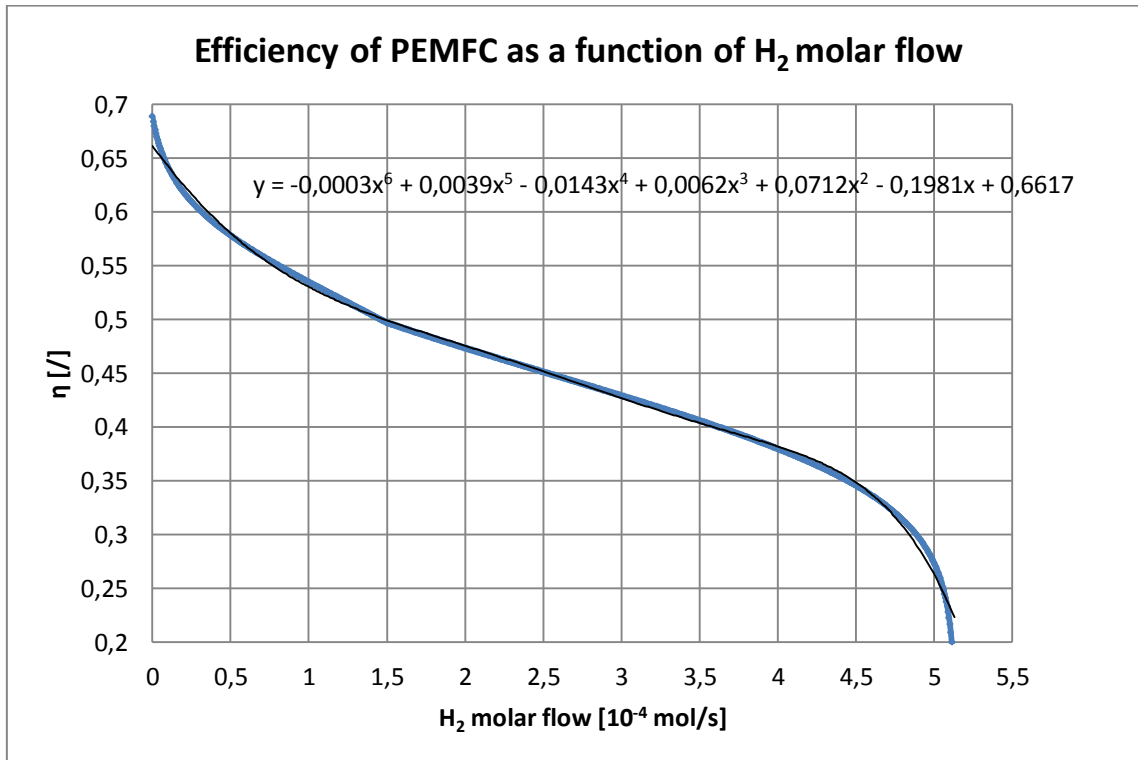
where  $d$  stands for thickness,  $A$  for active surface area and  $\sigma$  for proton conductivity of the membrane. It is assumed that all the other ohmic losses originating from stack components contact resistances are negligible.

At this point it needs to be mentioned that LT and HT PEMFC use the same characteristic curve for the stack efficiency even though it is clear that they will be different. Despite the fact that at higher temperature the equilibrium potential of PEMFC is lower the efficiency will be higher due to faster kinetics on the electrodes.

### 2.3 Combined system

Aspen Plus software was used to model a simplified system with the SMR and the PEMFC stack (low temperature – Figure 2, high temperature – Figure 3). In both cases the SMR operates at 250 °C and steam-to-methanol ratio = 1.5. The LT PEMFC stack operates at 90 °C, whilst the HT PEMFC stack operates at 250 °C. Because the temperature level of the system with the LT PEMFC stack is too low to be used for the endothermic reforming reaction an additional catalytic burner is needed to provide the sufficient heat to the SMR. In the system with LT PEMFC

partial heat regeneration is also used from hot exhaust gases exiting the reformer to the vaporiser of water methanol mixture.



Graph 1: Efficiency curve of PEMFC obtained from SIMULINK model

In presented SMR and PEMFC stack systems there are some assumptions and idealisations that need to be mentioned:

- adiabatic insulation of PEMFC stack and SMR
- ideal heat transfer between PEMFC stack and SMR (no losses)
- 100% methanol conversion in SMR
- 100% utilisation of hydrogen on anode side of PEMFC stack
- no scrubbing of gases exiting the reformer is considered (this is important particularly in the case of LT PEMFC CO poisoning)
- PEMFC stack operates at the same efficiency and nominal electric power of 25 W in both cases, the difference is only in the temperature level of generated heat



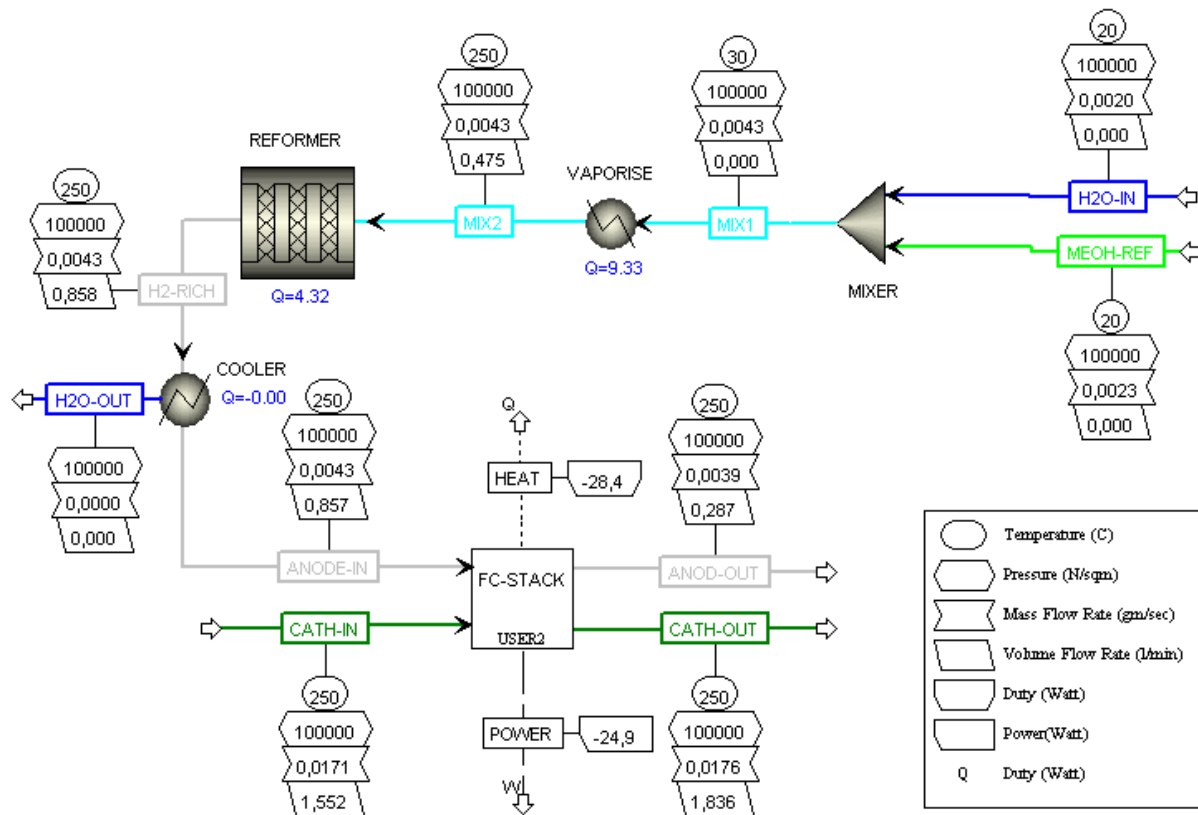
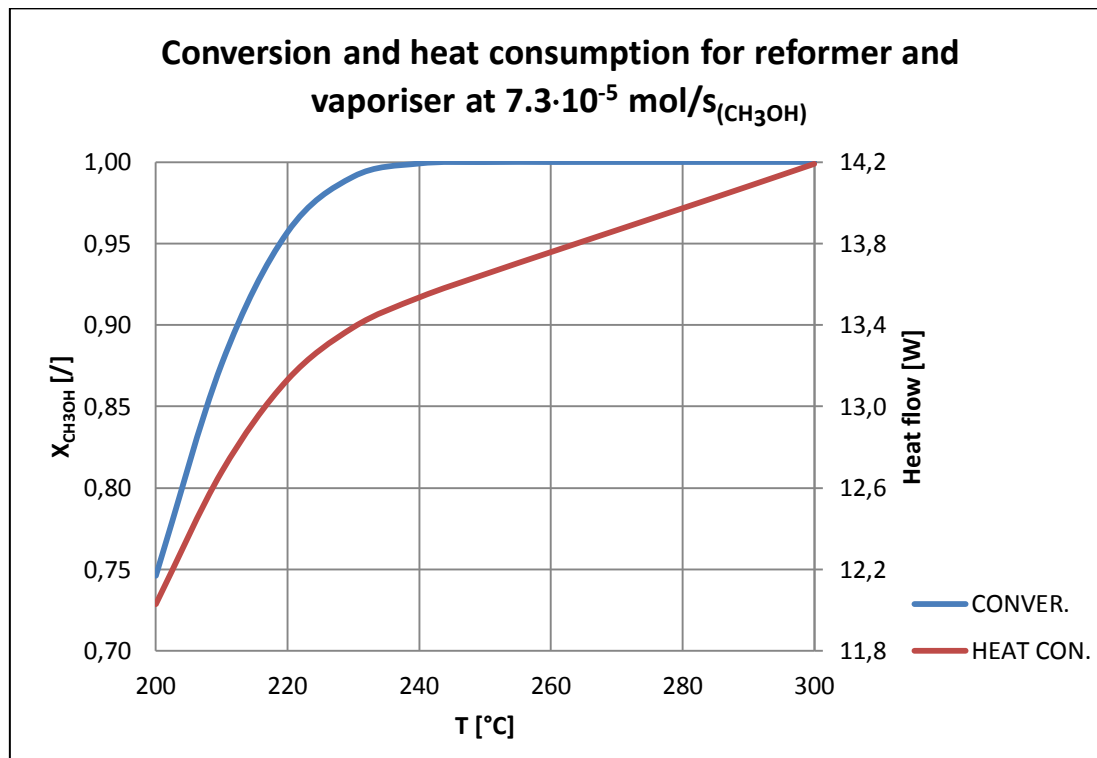


Figure 3: Mass and energy balance analysis of the system with SMR and HT PEMFC stack

Table 2: Conversion of methanol and heat flow needed in SMR and vaporizer as a function of temperature

T °C	X <sub>CH<sub>3</sub>OH</sub> /	Q̇ <sub>VAPORISER</sub> W	Q̇ <sub>REFORMER</sub> W	Q̇ W
200	0.7461	8.92	3.11	12.03
210	0.8761	9.00	3.68	12.68
220	0.9569	9.08	4.05	13.13
230	0.9910	9.17	4.22	13.39
240	0.9991	9.25	4.29	13.53
250	0.9999	9.33	4.32	13.65
260	1.0000	9.42	4.34	13.76
270	1.0000	9.50	4.36	13.87
280	1.0000	9.59	4.38	13.97
290	1.0000	9.67	4.41	14.08
300	1.0000	9.76	4.43	14.19



Graph 2: Methanol conversion and heat consumption as a function of operating temperature of the reformer

The blue line on Graph 2 shows the methanol conversion as a function of temperature at constant molar flow of  $7.3 \cdot 10^{-5} \text{ mol/s}$ . The model predicts that 100% conversion is achieved at temperatures above 240 °C. The red line shows the combined heat flow needed for the reforming reaction and vaporisation of methanol-water mixture at different operating temperatures of the reformer.

### 3.2 Comparison of LT and HT PEMFC Stack Systems

The comparison of both systems is quite straightforward because it is based on the assumptions stated in chapter 2.3. Nonetheless, it still allows a sufficiently accurate evaluation of the difference between both systems. The efficiency of an energy system is defined as stated in chapter 2.2 and with the use of Eq. (8) the following results are obtained:

$$\eta_{LT} = \frac{P}{\dot{m}_{LT} \cdot \Delta H_{HHV}} = \frac{25 \text{ W}}{0,033 \text{ g/s} \cdot 20 \text{ kJ/g}} = 37.9 \% , \quad (14)$$

$$\eta_{HT} = \frac{P}{\dot{m}_{HT} \cdot \Delta H_{HHV}} = \frac{25 \text{ W}}{0,023 \text{ g/s} \cdot 20 \text{ kJ/g}} = 54.3 \% , \quad (15)$$

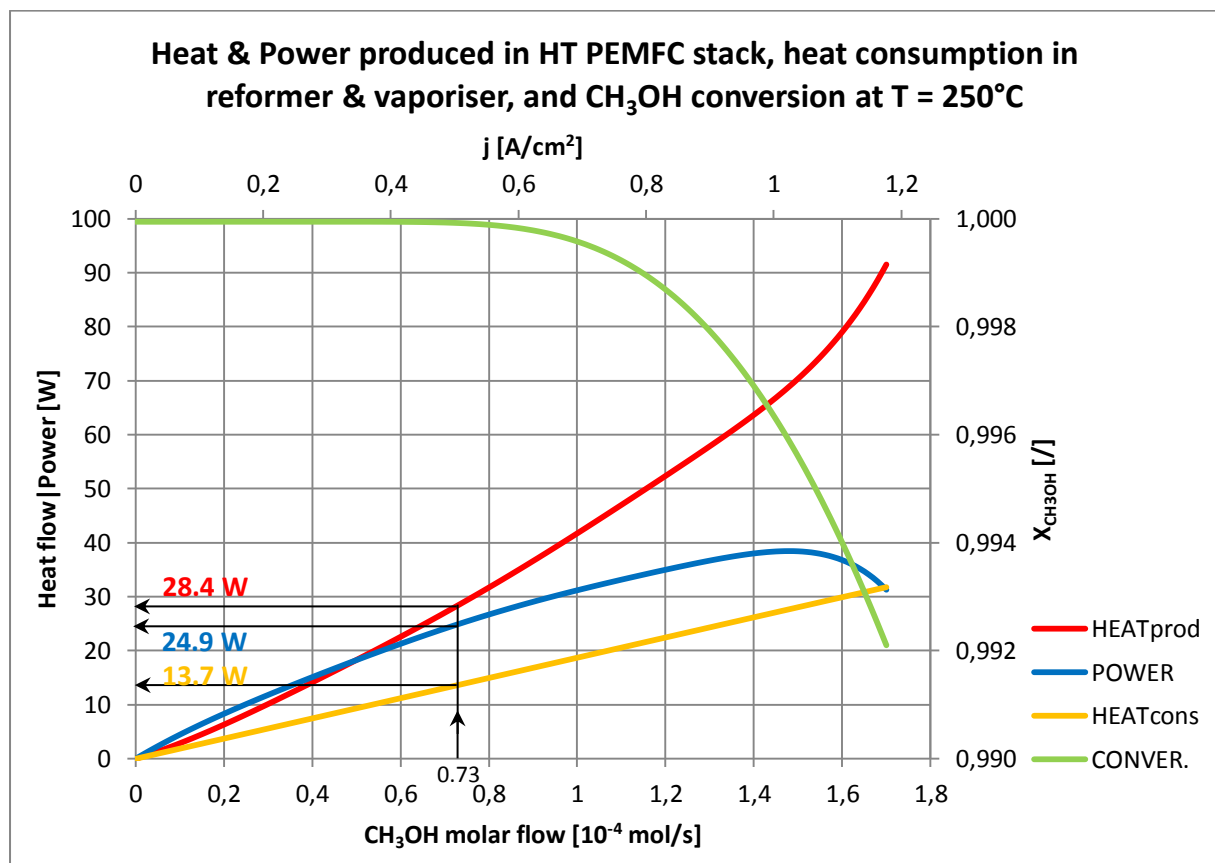
where  $\dot{m}$  is the molar flow of methanol and  $\Delta H_{HHV}$  the higher heating value of methanol. The calculations show that with the use of waste heat produced in electrochemical reaction the HT PEMFC system would have around 40% higher efficiency compared to the classical LT PEMFC system, where low level waste heat is in most cases useless.

The main characteristics of the two systems working at nominal operating point are given in Table 3. The cause of small difference in heat and power produced is in difference of the temperature of the reformat gas. Reformat gas entering the LT PEMFC stack at 90 °C has lower enthalpy and hence less energy is available to produce power and/or heat. The difference in consumed heat flow is only due to the heat regeneration of reformat gas; otherwise the same amount of heat is consumed in the SMR and vaporiser.

Table 3: Main characteristics of LT and HT PEMFC systems

Stack	Operating temperature	Power	Produced heat flow	Consumed heat flow	Additional heat flow	Efficiency
LT	90 °C	24.7 W	28.2 W	11.9 W	11.9 W	37.9%
HT	250 °C	24.9 W	28.4 W	13.6 W	0 W	54.3%

Sensitivity analysis of the HT PEMFC system as a function of methanol molar flow was performed. In that case the temperature of SMR and HT PEMFC was held constant at 250 °C.



Graph 3: Heat & Power produced in HT PEMFC, Heat consumption in reformer & vaporiser, and CH<sub>3</sub>OH conversion at T = 250 °C

On Graph 3 the red line represents the heat flow produced by the HT PEMFC, the blue line represents the power produced by the HT PEMFC and the orange line represents the heat flow needed to supply the SMR and the vaporiser. The green line represents the conversion of methanol where it can be seen that at molar flow  $7.3 \cdot 10^{-5}$  mol/s of methanol the reformer still achieves practically 100% conversion. Increasing the molar flow above this value reduces the conversion; however it is still well above 99% even at peak power of the HT PEMFC.

If nominal operating point is selected at conditions of methanol molar flow  $7.3 \cdot 10^{-5}$  mol/s and temperature 250 °C, the system produces 24.9 W of electricity, 28.4 W of heat flow and consumes 13.7 W of heat flow. Under the assumptions stated in chapter 2.3 this would mean that the system has the potential to produce more than twice as much heat as needed for the SMR and the vaporiser.

#### **4 Conclusions**

This study shows the feasibility of the HT PEMFC stack integration into a combined system with the SMR. The presented model of the system is based on certain idealised assumptions which will have to be changed when designing a real system. In this context a good isolation of such a system has to be provided and some temperature gradient will always be needed when heat is transferred. The SMR must be carefully designed to achieve high methanol conversion and also a proper design of the HT PEMFC stack is needed to achieve maximum utilisation of hydrogen. Nevertheless, the potential of the HT PEMFC stack stands in the use of a reformat fuel containing 2-3% of CO without downstream cleaning of hydrogen fuel.

Despite the idealised assumptions, the model demonstrates that such a system would achieve greater efficiency compared to a classical system with LT PEMFC stack. The use of high-level heat released during the electrochemical reaction would raise the efficiency of the system to 54.3% which is more than 40% higher compared to the LT PEMFC system.

It further demonstrates that the amount of heat released is twice as high as needed in the system. This means that there is still a lot of heat available to be used in other cogeneration processes that would increase the efficiency of the system even further. For example, this heat can be used in combination with thermoelectric modules (reverse Peltier element) to produce additional electric power.

#### **5 Acknowledgements**

This work is a part of on-going projects financed by Slovenian MoD (Contract No. 4300-434/2010-1) and by Centre of Excellence Low Carbon Technologies (CoE LCT).

#### **6 References**

- [1] Basu, Suddhasatwa. Recent Trends in Fuel Cell Science and Technology. Dordrecht : Springer, 2007.
- [2] Peppley, Brant A., et al. Methanol-steam reforming on Cu/ZnO/Al<sub>2</sub>O<sub>3</sub> catalysts. Part 2. A comprehensive kinetic model. Applied Catalysis A: General. 1999, Vol. 179, pp. 31-49.



19 – 20 June 2012  
Brussels, Belgium

**Military Green 2012**  
Conference-Exhibition-Demonstration  
*Call for Exhibits and Demonstrations*



- [3] Pattekar, Ashish V. and Kothare, Mayuresh V. A Radial Microfluidic Fuel Processor. *Journal of Power Sources*. 2005, Vol. 147, pp. 116-127.
- [4] Telotte, John C., Kern, Jesse and Palanki, Srinivas. Miniaturized Methanol Reformer for Fuel Cell Powered Mobile Applications. *International Journal of Chemical Reactor Engineering*. 2008, Vol. 6, Article A64.